

Fallout plume of submerged oil from *Deepwater Horizon*

David L. Valentine^{a,b,1}, G. Burch Fisher^{a,b}, Sarah C. Bagby^{a,b}, Robert K. Nelson^c, Christopher M. Reddy^c, Sean P. Sylva^c, and Mary A. Woo^d

^aDepartment of Earth Science and ^bMarine Science Institute, University of California, Santa Barbara, CA 93106; ^cDepartment of Marine Chemistry and Geochemistry, Woods Hole Oceanographic Institution, Woods Hole MA 02543; and ^dDepartment of Earth System Science, University of California, Irvine, CA 92697

Edited by Derek C. G. Muir, Environment Canada, Burlington, ON, Canada, and accepted by the Editorial Board September 26, 2014 (received for review August 5, 2014)

The sinking of the *Deepwater Horizon* in the Gulf of Mexico led to uncontrolled emission of oil to the ocean, with an official government estimate of ~5.0 million barrels released. Among the pressing uncertainties surrounding this event is the fate of ~2 million barrels of submerged oil thought to have been trapped in deep-ocean intrusion layers at depths of ~1,000–1,300 m. Here we use chemical distributions of hydrocarbons in >3,000 sediment samples from 534 locations to describe a footprint of oil deposited on the deep-ocean floor. Using a recalcitrant biomarker of crude oil, 17 α (H),21 β (H)-hopane (hopane), we have identified a 3,200-km² region around the Macondo Well contaminated by $\sim 1.8 \pm 1.0 \times 10^6$ g of excess hopane. Based on spatial, chemical, oceanographic, and mass balance considerations, we calculate that this contamination represents 4–31% of the oil sequestered in the deep ocean. The pattern of contamination points to deep-ocean intrusion layers as the source and is most consistent with dual modes of deposition: a “bathtub ring” formed from an oil-rich layer of water impinging laterally upon the continental slope (at a depth of ~900–1,300 m) and a higher-flux “fallout plume” where suspended oil particles sank to underlying sediment (at a depth of ~1,300–1,700 m). We also suggest that a significant quantity of oil was deposited on the ocean floor outside this area but so far has evaded detection because of its heterogeneous spatial distribution.

Macondo Well blowout | Gulf of Mexico | ocean pollution | petroleum spill | deep plumes

The sinking of the *Deepwater Horizon* in the Gulf of Mexico led to the discharge of ~5.0 million barrels of petroleum from the Macondo Well. The discharge occurred at a water depth of ~1,500 m and gave rise to intrusion layers (1) in the deep ocean that included both water-soluble hydrocarbons in the dissolved phase (2–6) and small particles of water-insoluble hydrocarbons (7–11). These intrusion layers were found primarily at a depth of 1,000–1,300 m and may have hosted the majority of the environmental discharge, including all the natural gas and ~2 million barrels of liquid oil (12). Although the most abundant of the water-soluble hydrocarbons underwent rapid biodegradation during the spill (4, 6, 8, 9, 13–15), the fate and impacts of the insoluble hydrocarbons in the deep ocean have remained uncertain (16).

The intrusion layers that hosted hydrocarbon contamination persisted for 6 mo or more and at distances >300 km from the well, but available evidence suggests that particles of submerged oil were particularly concentrated during the first 6 wk of discharge and within ~15 km of the well (8, 9, 11). Thus, initial partitioning of hydrocarbon particles to the intrusion layers appears to have given way to transport or removal by undefined deep-ocean processes. Such processes might include sedimentation, buoyant rise toward the sea surface, incorporation into pelagic biota, biodegradation, or interventions at the wellhead. Mechanisms exist that support several of these options (9, 17–20), but uncertainty as to oil’s actual partitioning, the effect of chemical dispersant (21), and the impacts of a changing

microbial community (6, 8, 9, 13–15, 17, 22–24) have precluded further understanding of the processes that acted on the oil.

In this study we focus on testing the hypothesis that oil particles suspended in the deep intrusion layers were deposited on the sea floor over a broad area. To do so, we use publicly available data generated as part of the ongoing Natural Resource Damage Assessment (NRDA) process (*Supporting Information*) to assess the spatial distribution of petroleum hydrocarbons in the deep-ocean sediments of the Gulf of Mexico. We focus on the recalcitrant compound 17 α (H),21 β (H)-hopane (hereafter referred to as “hopane”) as a conserved tracer for crude oil deposition to sediments (25); we treat hopane as a degradation-resistant proxy for Macondo’s liquid-phase oil (26). Analysis of the spatial distribution of hopane allows us to define both a regional background level and a depositional footprint of oil from the *Deepwater Horizon* event. In combination with other lines of evidence, this analysis leads us to conclude that significant quantities of particulate oil sank from the intrusion layers to rest on the underlying sea floor.

Results and Discussion

Hopane Distribution Is Consistent with Macondo as the Source. Our first goal was to determine if the distribution of hopane in the Gulf of Mexico’s deep-water sediments could be used quantitatively as a tracer of Macondo discharge. Because hopane is not unique to Macondo Well oil, we investigated its spatial distribution (Fig. 1) for indications of its origin. To help determine

Significance

Following the sinking of the *Deepwater Horizon* in the Gulf of Mexico an unprecedented quantity of oil irrupted into the ocean at a depth of 1.5 km. The novelty of this event makes the oil’s subsequent fate in the deep ocean difficult to predict. This work identifies a fallout plume of hydrocarbons from the Macondo Well contaminating the ocean floor over an area of 3,200 km². Our analysis suggests the oil initially was suspended in deep waters and then settled to the underlying sea floor. The spatial distribution of contamination implicates accelerated settling as an important fate for suspended oil, supports a patchwork mosaic model of oil deposition, and frames ongoing attempts to determine the event’s impact on deep-ocean ecology.

Author contributions: D.L.V., R.K.N., C.M.R., S.P.S., and M.A.W. designed research; D.L.V., G.B.F., and S.C.B. analyzed data; and D.L.V. wrote the paper.

The authors declare no conflict of interest.

This article is a PNAS Direct Submission. D.C.G.M. is a guest editor invited by the Editorial Board.

Freely available online through the PNAS open access option.

¹To whom correspondence should be addressed. Email: valentine@geol.ucsb.edu.

This article contains supporting information online at www.pnas.org/lookup/suppl/doi:10.1073/pnas.1414873111/-DCSupplemental.

whether hopane originated from the Macondo Well, we asked whether its distribution was consistent with the *Deepwater Horizon* event across three spatial scales. That is, for a given core, is the hopane concentration higher in the surficial layer of sediment than in underlying sediment, as would be expected for recent deposition? For a given sampling site, do surficial hopane concentrations vary widely from core to core, as would be expected for particle deposition? For the region, is hopane concentration elevated close to the Macondo Well, as might be expected for proximity to an intense point source?

To assess whether hopane in surficial sediments (i.e., the uppermost 1 or 2 cm of the sediment that makes up the sea floor) originated from recent deposition, we assessed its depth distribution in sediment cores for which complete depth profiles were available. Cores were binned by expedition to retain consistent sample intervals; data were normalized to the surface layer (=100%) for each core and binned by surficial hopane concentration to establish a baseline trend (*Supporting Information*). Cores with surficial hopane concentrations of $<25 \text{ ng}\cdot\text{g}^{-1}$ show a slight linear decrease in hopane concentration with sediment depth, providing no indication of recent deposition, but the hopane profile in cores with higher surficial concentrations is best fit by an exponential decay curve (Fig. 2), suggesting recent anomalous hopane deposition in these cores. The 323 cores with the highest ($>100 \text{ ng}\cdot\text{g}^{-1}$) levels of surficial hopane, collected during eight expeditions, follow this pattern with notable consistency (Fig. 2A).

Next, we examined the variability of surficial hopane concentrations in sets of cores collected in parallel. These measurements frequently ranged over one to two orders of magnitude at a single sampling site (Fig. S1). We used surficial hopane concentrations to develop a quantitative particle deposition model and asked whether the model could explain the high degree of variation observed. Because little is known of the likely distribution of oil masses carried by depositing particles, we used Monte Carlo methods to fit particle number and oil mass to the measured distribution of surficial hopane concentration (Figs. S2 and S3). This multimodal distribution was best fit by deposition at a spatial density of 228 particles/m², with 88% of particles bearing an average (unweathered) oil mass of 0.024 g each, 10% bearing an average oil mass of 0.19 g, and 2% bearing an average oil mass of 1.13 g (mean hopane masses of 1.4, 11, and 65 μg , respectively; see *Supporting Information* for details). We then used this model to simulate 2 m \times 2 m patches of seafloor, selected two to five positions at random in each patch for “coring,” and calculated (i) the surficial hopane concentration that would result from the particles deposited within each simulated core’s cross-section and (ii) the mean and SD of these concentrations for each simulated site. Finally, for each sample site in the Gulf

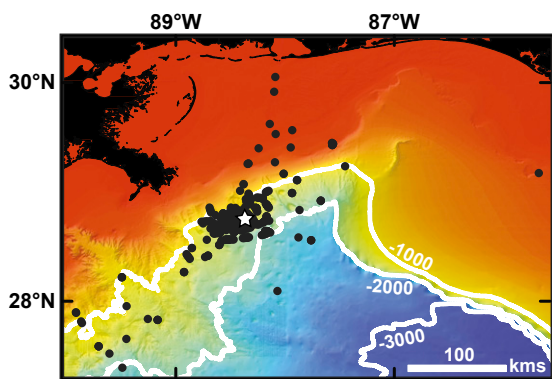


Fig. 1. Map of the northern Gulf of Mexico showing the sampling locations (black dots) and the Macondo Well (white star) overlaid on the National Geophysical Data Center Coastal Relief Model bathymetry.

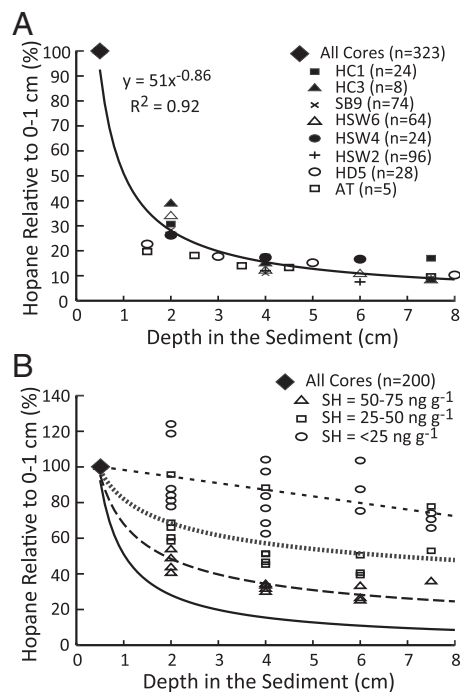


Fig. 2. Depth distributions of hopane concentration. (A) Hopane’s depth distribution relative to the surficial layer (0–1 cm) for sediments with surficial hopane (SH) $>100 \text{ ng}\cdot\text{g}^{-1}$. The data are given as the midpoint depth for each sediment interval and as the mean value for each sampling expedition as indicated. (B) Hopane’s depth distribution relative to the surficial layer (0–1 cm) for sediments with surficial hopane concentrations of $<25 \text{ ng}\cdot\text{g}^{-1}$, 25–50 $\text{ng}\cdot\text{g}^{-1}$, and 50–75 $\text{ng}\cdot\text{g}^{-1}$. The data are in the same form as in A. Regressions are fit to the data, from top to bottom, as follows: SH $<25 \text{ ng}\cdot\text{g}^{-1}$ ($y = -3.7x + 102$; $R^2 = 0.31$); SH = 25–50 $\text{ng}\cdot\text{g}^{-1}$ ($y = 82x^{-0.26}$, $R^2 = 0.62$); SH = 50–75 $\text{ng}\cdot\text{g}^{-1}$ ($y = 68x^{-0.49}$, $R^2 = 0.93$). The solid curve at bottom (SH $>100 \text{ ng}\cdot\text{g}^{-1}$) is from A and is provided for visual reference. Additional information is available in [Dataset S1](#).

of Mexico at which parallel cores were collected, we calculated the mean and SD of measured surficial hopane concentrations. The within-site variation as measured in parallel cores was in very good agreement with simulated values (Fig. 3), indicating that sparse deposition of heterogeneous oil-bearing particles is sufficient to explain the frequent coexistence of highly contaminated spots alongside spots with low hopane concentration.

To assess whether surficial hopane was elevated in the vicinity of the Macondo Well, we analyzed its spatial distribution for all available locations as a function of the radial distance from the Macondo Well and the sea floor depth. The results shown in Fig. 4 and Fig. S4 indicate a mean concentration for surficial hopane of $28 \pm 23 \text{ ng}\cdot\text{g}^{-1}$ ($n = 70$) for locations $>40 \text{ km}$ from the Macondo Well, providing an estimate for the mean background concentration (see *Supporting Information* for additional details). Only 3% of sampling sites at this distance from the well contained surficial hopane concentrations $>75 \text{ ng}\cdot\text{g}^{-1}$ (Fig. 4A and Fig. S4), whereas 68% (314 of 464) of locations within 40 km of the Macondo Well contained surficial hopane at $>75 \text{ ng}\cdot\text{g}^{-1}$, providing an estimate for the upper limit of background concentrations. The concentration of surficial hopane depended on sea floor depth (Fig. 4B and C), with peak values at 1,300–1,600 m, bracketed by lower but still elevated concentrations at 900–1,300 and 1,600–1,700 m. Outside these depths and within 40 km of the Macondo Well only 17% of locations (9 of 54) contained surficial hopane concentrations $>75 \text{ ng}\cdot\text{g}^{-1}$, compared with 74% of samples (303 of 410) within this depth range and within 40 km of the Macondo Well. This basin-scale analysis provides an

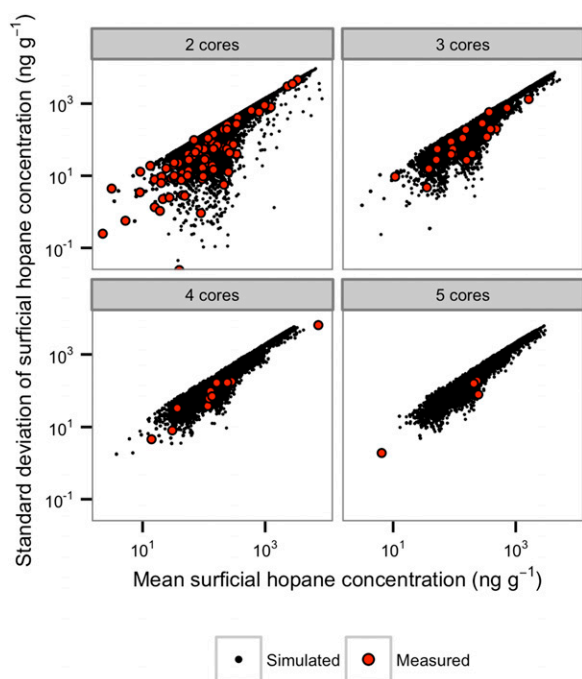


Fig. 3. Comparison of measured variation in surficial hopane concentrations within sampling sites (red dots) and modeled variation within simulated sampling sites (black dots). Within-site variability was assessed in the particle deposition model by simulating deposition on a patch of sediment, randomly sampling two, three, four, or five nonoverlapping loci with the same cross-sectional area as standard push-cores, calculating the hopane signal that would result from the combination of background signal and oil particles captured within each locus, and comparing the results across loci within the same simulated site.

estimate of $28 \text{ ng}\cdot\text{g}^{-1}$ for the mean background concentration of surficial hopane and a threshold of $75 \text{ ng}\cdot\text{g}^{-1}$ for distinguishing between background surficial hopane and hopane contamination and further defines a clear regional anomaly that is highly pronounced within 40 km of the Macondo Well and at depths of 900–1,700 m.

Collectively, these analyses of the distribution of hopane concentration in the Northern Gulf of Mexico across multiple spatial scales suggest a recent, intense, and heterogeneous depositional event centered near the Macondo Well. Based on this evidence and the magnitude of discharge during the event, we attribute the excess hopane observed in surficial sediments to discharge from the Macondo Well and propose that this hopane anomaly be used as a proxy for liquid oil from the spill.

Extent and Pathway of Hopane Deposition. The second goal of this study was to quantify the depositional footprint of the spill and identify pathways by which the oil might have deposited. Toward this goal we posed several questions. What fraction of hopane discharge resides in the contaminated zone? Is the spatial distribution of surficial hopane contamination consistent with a source from the deep intrusion layers? Does the pattern of contamination provide insight as to the oil's depositional pathway?

To estimate the magnitude of emitted hopane deposited to the sea floor within the defined contaminated area, we used multiple approaches (Tables S1–S4) to interpolate the total surficial hopane contamination load from surficial hopane concentration measurements. With the assumption that the mean background concentration is $28 \pm 23 \text{ ng}\cdot\text{g}^{-1}$, our preferred method of calculation yields a total load for surficial hopane contamination of $1.8 \pm 1.0 \times 10^6 \text{ g}$, which represents $\sim 6 \pm 5\%$ of the hopane emitted to the environment from the Macondo Well;

we take the lowest estimate minus one SD as a lower bound and the highest estimate plus one SD as an upper bound, yielding a range of 0.7×10^6 to $3.4 \times 10^6 \text{ g}$. Assuming that 2 ± 0.2 million barrels of oil remained trapped at depth (12), these calculations represent, by proxy, $\sim 12\%$ (range, 4–31%) of the oil trapped in the deep intrusion layers. We view this estimate as a lower bound for the region investigated because three reservoirs of hopane contamination are missing from the calculation: (i) sediments beneath the surficial layer (Fig. 2B); (ii) the water overlying core samples upon collection; and (iii) sediments in the debris field that include splays of drilling mud from the failed top-kill operation. Furthermore, the identified contamination represents a minimum area, because the spatial extent was truncated for areas of low sample density. Because hopane is used as a proxy for oil, the estimate does not account for biodegradation or dissolution of other petroleum hydrocarbons.

To assess further the spatial distribution of hopane contamination, we contoured the concentration of surficial hopane in an area of $3,200 \text{ km}^2$ for which we had sufficient data coverage ($n = 461$ locations). Fig. 5 displays results from an empirical Bayesian kriging method (other methods provided similar results; see [Supporting Information](#)) and reveals an oblong patchwork of contamination that trends primarily to the west from the Macondo Well to a distance of at least 40 km. The observed pattern is consistent with the mixing and deep-ocean currents during the event (24, 27, 28), although we identified less oil to the east than would be expected from current patterns. Comparing the observed deposition pattern with the region's bathymetry reveals moderate hopane contamination along the continental slope at sea floor depths of 900–1,300 m, the depths at which hydrocarbon intrusion layers were reported (2–4, 7, 9), and a stronger hopane anomaly at depths of 1,300–1,600 m (Figs. 4 and 5). Although the contamination at 900–1,300 m is consistent with a bathtub-ring mechanism of deposition, the heavier contamination below suggests that fallout from the intrusion layers was more important. The observed distribution of hopane contamination implicates the intrusion layers rather than the sea surface as the likely source of oil to deep-ocean sediments.

To distinguish better between deposition from the intrusion layers and deposition from the sea surface, we used hopane's distribution to anchor analysis of two other datasets: the footprint for surface oil slicks as observed by remote sensing during the time of discharge (29) and the spatial distribution of several volatile hydrocarbons present at contaminated locations. These datasets have the potential to discriminate between two possible modes of deposition: mode 1, sedimentation of oil that was released from the Macondo Well and trapped in the ocean's interior without ever being exposed to the atmosphere; and mode 2, sedimentation of Macondo oil from the sea surface to the sea floor [the sinking of oil-laden particles from the sea surface popularly referred to as “the dirty blizzard” (16), by analogy with natural marine snow]. We first compared the footprint of the observed hopane anomaly with the footprint for surface oil slicks. Together with rapid surface transport (30, 31) and slower transport of the deep plumes (32), the profound mismatch in these footprints (Fig. 6A) argues against the sea surface (mode 2) as the major source of deposition. We then analyzed the spatial distribution of several volatile hydrocarbons present at a subset of contaminated locations (i.e., with surficial hopane concentrations $>75 \text{ ng}\cdot\text{g}^{-1}$). Volatile hydrocarbons are lost to evaporation rapidly when oil is exposed to the atmosphere; thus, the presence of undecane (Fig. S5) and hexadecane (Fig. 6B) at 51 and 65 of these locations, respectively, indicates that oil in these samples was not exposed to extensive weathering in surface slicks (10), again arguing against mode 2 deposition. Similarly, the ratio of pristane to phytane (1.63–1.99 in Macondo oil) (5, 33) drops with extensive weathering; previous work with Macondo oil has found values as low as 1.16 for moderately weathered

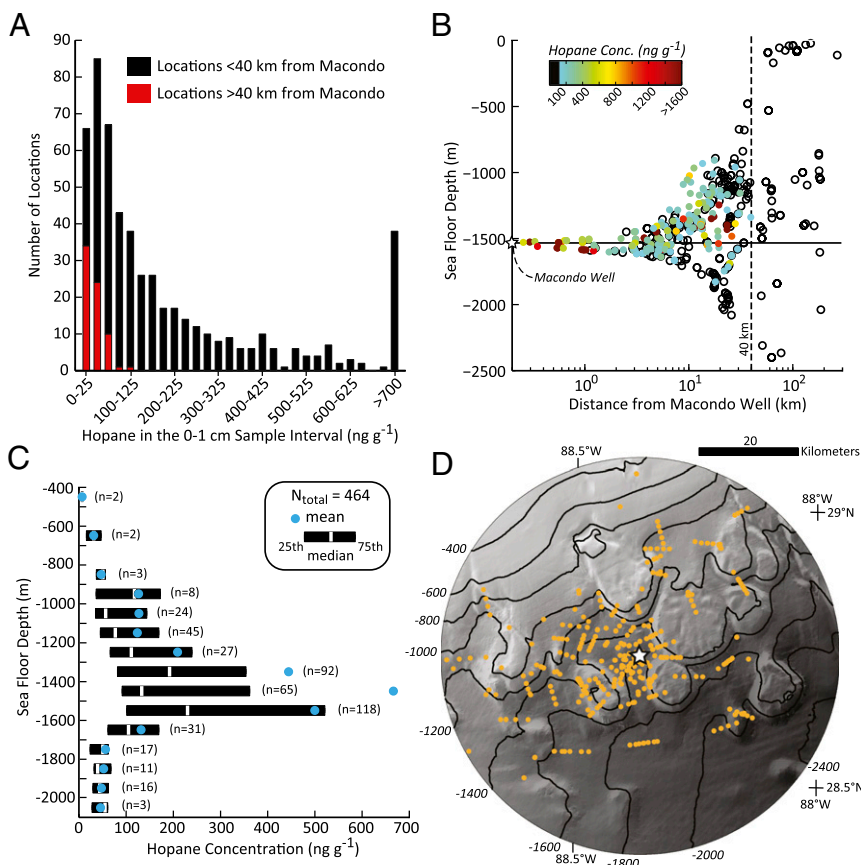


Fig. 4. Spatial distribution and concentrations of hopane in surficial sediments. (A) Histogram of all surficial hopane samples ($n = 534$) binned by concentration. (B) Plot of data from A with respect to sea floor depth and distance from the Macondo Well and colored by hopane concentration. Twenty-one samples have concentrations $>1,600 \text{ ng g}^{-1}$ with a maximum concentration of $12,800 \text{ ng g}^{-1}$. (C) Box plot showing the depth distribution of surficial hopane concentration for all locations within a 40-km radius of the Macondo Well. The median (white bars), mean (blue dots), and 25th and 75th percentile confidence limits (black box) are shown for samples binned by 100-m sea floor depth intervals. (D) Map view of all sample locations within 40 km of the Macondo Well (orange dots and white star, respectively) as plotted in C, with 200-m bathymetry contour intervals shown (black lines).

slicks (33), 0.11 for thin slicks after several hours of weathering (34), and 0.29 for floating debris (35). We determined the pristane:phytane ratio for the 84 available locations, finding a median value of 1.68 (mean = 2.2, SD = 1.8), with only one value below 0.97. The similarity between these ratios and the value for Macondo oil again suggests mainly mode 1 deposition. None of the lines of evidence presented here absolutely excludes a contribution from mode 2 deposition, but all support the claim that the observed hopane anomaly (Fig. 5) was derived primarily

from the fraction of Macondo oil that initially was suspended as intrusion layers in the ocean's interior.

Implications and Mechanisms. The results of this work identify a fallout plume of hopane from the *Deepwater Horizon* event that spans an area of $3,200 \text{ km}^2$ and by proxy represents 4–31% of the oil estimated to have been trapped in the deep ocean. Beyond this finding, the results carry several notable implications and provide insight as to the mechanism of mode 1 oil deposition.

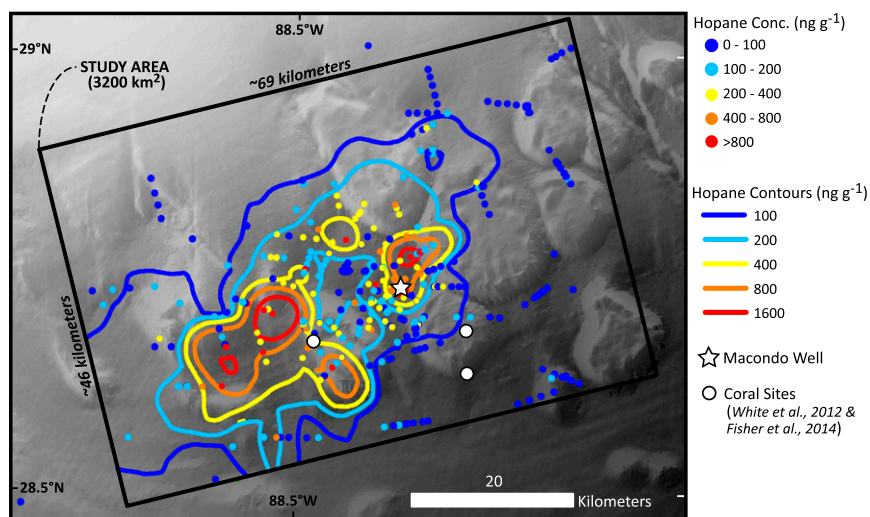


Fig. 5. Interpolated hopane contours generated using empirical Bayesian kriging (EBK) for surface C (EBK-C; Figs. S6–S8 and Table S4) and overlaid on measured hopane concentrations and regional bathymetry (see Supporting Information for details of the interpolation parameters and techniques).

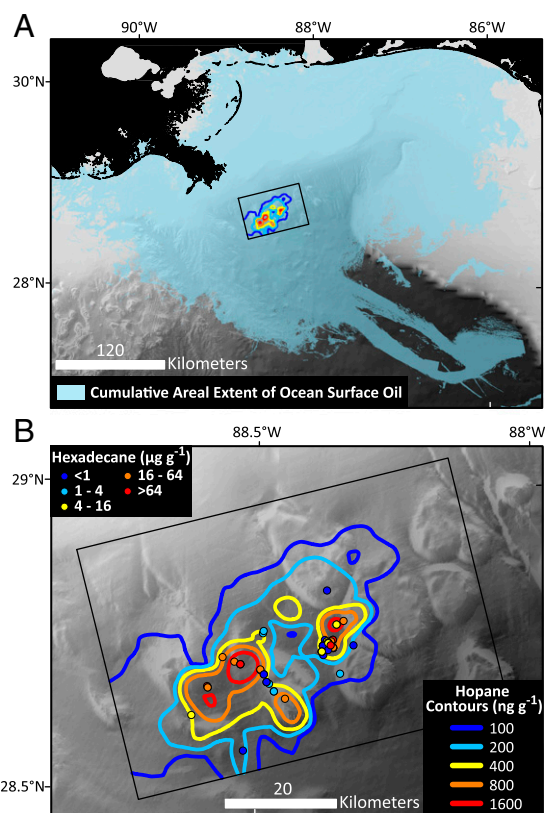


Fig. 6. Spatial and chemical evidence supporting mode 1 deposition. (A) Cumulative areal extent of ocean surface oil (blue) detected using Synthetic Aperture Radar with a Textural Classifier Neural Network Algorithm (TCNNA) from April to mid-August, 2010 (29). The study area and hopane contours from Fig. 5 are shown along with bathymetry and the Gulf Coast (black). (B) Concentration of hexadecane overlaid on the interpolated hopane contours and study area from Fig. 5 ($n = 65$).

The combination of a patchy distribution at the regional scale (Fig. 5 and Figs. S6–S8) with the heterogeneity observed at the meter-long scale (Fig. 3 and Figs. S1–S3) lead us to a conceptual view of the oil's distribution as a patchwork mosaic. This framework provides hints about the location of as yet unidentified deposits. That is, based on a model of settling oil particles or floc (17, 20), we predict that deposition of similarly sized particles occurred over an area much greater than 3,200 km², but that the average distance between deposited particles increased in proportion to the radial arc from the Macondo Well. Increased distance between deposited particles would reduce the probability of finding Macondo oil within any given sediment core, so that the sparser sampling performed away from the wellhead is unlikely to have captured the full extent of contamination.

For oil to sink from the deep intrusion layers to the sea floor, oil particles must overcome the ambient hydrodynamic forces holding them in suspension, most likely by increasing in size and density. What process(es) might cause these changes? A mechanism for accelerated settling has yet to be defined adequately but must differ from processes at the sea surface (20), because suspension at depth precludes both evaporative weathering and accumulation at an air–sea interface. The results presented here do not define a mechanism, but in combination with the published literature (6, 8, 9, 15, 17, 36) they lead us to hypothesize that bacterial blooms driven primarily by consumption of soluble hydrocarbons produced biomass that acted as flocculant to capture suspended hydrocarbon particles. Oily bacterial flocs

could have increased in size by accretion and/or continued bacterial growth on aqueous-phase hydrocarbons; floc density could have increased by this accumulation of dense bacterial biomass/biofilms combined with the selective biodegradative loss of lighter hydrocarbons from the particulate phase. Estimations of particle oil content indicate the accretion of 10⁴–10⁷ smaller particles (with an initial size of 50–100 µm) before sinking (Table S5). This mechanism of accelerated settling fulfills both the size and density requirements, is consistent with the flocculation of *Colwellia* (17), and generally is consistent with the patchwork mosaic model of deposition. Such aggregation seemingly counters the effect of dispersant, and the underlying mechanism remains a speculative unknown. Based on this hypothesis we suggest that feedback between microbial blooms and oil deposition could have modulated the intensity and location of deposition.

The spatial distribution of above-background surficial hopane defines a contaminated area that frames interpretations of the resulting ecological damage. For example, potentially damaged deep-sea corals (37) lie within the contaminated region to the southwest of the Macondo Well (Fig. 5). Our analyses indicate that significant quantities of Macondo oil were transported near the corals before or during fallout to the sediment. Deposition of oil in the vicinity of the coral community provides a route to exposure, which has been a topic of contention (37–39). Two additional impacted coral communities (40) to the southeast also lie within the contaminated region (Fig. 5). As a second example, the ecological damage to soft-bottom benthic communities (e.g., a reduction in macrofaunal and meiofaunal diversity and an increase in the nematode-to-copepod ratio) from Macondo oil might mirror the patchwork mosaic pattern of contamination. Accepted approaches to assess ecological damage to the deep benthos include collecting chemical and ecological data from parallel cores. However, the mosaic pattern of oil deposition may complicate such an assessment because of the heterogeneity expected at this spatial scale (Fig. 3 and Fig. S1). We predict this mosaic effect would become more pronounced as particle spatial density decreases with increasing distance from the Macondo Well, potentially explaining why such ecological impacts are more clearly apparent at close proximity to the well (41).

Finally, the identification of hopane contamination from *Deepwater Horizon* in surficial sediments provides a conservative benchmark to which other hydrocarbons can be compared. This approach provides a path to study the physical processes that acted on the oil particles and to assess in situ rates of hydrocarbon biodegradation.

Methods

The data used in this study were collected and released through the NRDA process, overseen by the National Oceanic and Atmospheric Administration (NOAA). All data are publicly available from NOAA and were downloaded on January 1, 2014 from www.gulfspillrestoration.noaa.gov/oil-spill/gulf-spill-data/. We included all samples from the offshore environment available for download by January 1, 2014. We then selected the subset of samples that included data for hopane concentration measured in the surficial sediment (top 1 or 2 cm, referred to here as “surficial hopane”). A total of 549 stations met this criterion for inclusion. We excluded 15 of these stations because the concentration of hopane increased markedly with depth, indicating long-term inputs consistent with natural oil seepage, although this approach is conservative and may exclude physically mixed samples containing Macondo oil. Replicate samples were collected at 117 of the 534 stations as follows: two samples were collected at each of 81 stations, three samples were collected at each of 21 stations, four samples were collected at each of 11 stations, and five samples were collected at each of four stations. For stations where multiple samples were collected, the average value was used to represent the hopane concentration at that station, but samples were considered individually for other analyses. Hopane concentration was below detection in the surficial sediments at 11 of the 534 stations. The samples originated from 12 expeditions as follows: Pisces Cruise 6 (P6; 25 September–5 October 2010); HOS Davis Cruise 3 (HD3; 8–28 September 2010); HOS Davis

Cruise 5 (HD5; 4–18 December 2010); Atlantis Cruise (AT; 4–15 December 2010); HOS Sweetwater Cruise 1 (HSW1; 10–13 March 2011); HOS Sweetwater Cruise 2 (HSW2; 23 March–24 April 2011); Sarah Bordelon Cruise 9 (SB9; 23 May–13 June 2011); HOS Sweetwater Cruise 4 (HSW4; 14 July–7 August 2011); HOS Sweetwater Cruise 6 (HSW6; 24 August–2 September and 29 September–21 October 2011); Holiday Chouest Cruise 1 (HC1; 25 August–13 September 2011); Holiday Chouest Cruise 2 (HC2; 15–30 September 2011); and Holiday Chouest Cruise 3 (HC3; 1–25 October 2011). Stations are identified in Fig. 1 and in *Supporting Information*.

Hopane concentration was measured as nanograms of hopane per gram of dry sediment. To integrate the hopane concentration spatially, we first calculated the average mass of dry sediment per unit volume of total sediment for available samples of the surface layer. Using an average sediment mass fraction (\pm SD) of 0.31 (\pm 0.13) ($n = 1,091$) and a particle density of 2.65 g/cm³ (42), we calculate an average sediment mass of 0.38 \pm 0.16 g/cm³ of total sediment. These values equate to a sediment porosity of 0.86 \pm 0.06, which is within the range typically observed for sediment core tops in the Gulf of Mexico (43). We then multiplied the specific density value of 0.38 \pm 0.16 g/cm³ by the volume of the study area (3.2×10^{13} cm² \times 1 cm depth interval) and the average excess of hopane, 1.51 \pm 0.23 $\times 10^{-7}$ g(hop)/g(sed) [range, 1.2–2.0 $\times 10^{-7}$ g(hop)/g(sed)]

- Socolofsky SA, Adams EE, Sherwood CR (2011) Formation dynamics of subsurface hydrocarbon intrusions following the Deepwater Horizon blowout. *Geophys Res Lett* 38(9):L09602.
- Diercks AR, et al. (2010) Characterization of subsurface polycyclic aromatic hydrocarbons at the Deepwater Horizon site. *Geophys Res Lett* 37(20):L20602.
- Joye SB, MacDonald IR, Leifer I, Asper V (2011) Magnitude and oxidation potential of hydrocarbon gases released from the BP oil well blowout. *Nat Geosci* 4(3):160–164.
- Kessler JD, et al. (2011) A persistent oxygen anomaly reveals the fate of spilled methane in the deep Gulf of Mexico. *Science* 331(6015):312–315.
- Reddy CM, et al. (2012) Composition and fate of gas and oil released to the water column during the Deepwater Horizon oil spill. *Proc Natl Acad Sci USA* 109(50):20229–20234.
- Valentine DL, et al. (2010) Propane respiration jump-starts microbial response to a deep oil spill. *Science* 330(6001):208–211.
- Camilli R, et al. (2010) Tracking hydrocarbon plume transport and biodegradation at Deepwater Horizon. *Science* 330(6001):201–204.
- Dubinsky EA, et al. (2013) Succession of hydrocarbon-degrading bacteria in the aftermath of the deepwater horizon oil spill in the gulf of Mexico. *Environ Sci Technol* 47(19):10860–10867.
- Hazen TC, et al. (2010) Deep-sea oil plume enriches indigenous oil-degrading bacteria. *Science* 330(6001):204–208.
- Ryerson TB, et al. (2012) Chemical data quantify Deepwater Horizon hydrocarbon flow rate and environmental distribution. *Proc Natl Acad Sci USA* 109(50):20246–20253.
- Spier C, Stringfellow WT, Hazen TC, Conrad M (2013) Distribution of hydrocarbons released during the 2010 MC252 oil spill in deep offshore waters. *Environ Pollut* 173:224–230.
- McNutt MK, et al. (2012) Review of flow rate estimates of the Deepwater Horizon oil spill. *Proc Natl Acad Sci USA* 109(50):20260–20267.
- Lu Z, et al. (2012) Microbial gene functions enriched in the Deepwater Horizon deep-sea oil plume. *ISME J* 6(2):451–460.
- Mason OU, et al. (2012) Metagenome, metatranscriptome and single-cell sequencing reveal microbial response to Deepwater Horizon oil spill. *ISME J* 6(9):1715–1727.
- Redmond MC, Valentine DL (2012) Natural gas and temperature structured a microbial community response to the Deepwater Horizon oil spill. *Proc Natl Acad Sci USA* 109(50):20292–20297.
- Schrope M (2013) Dirty blizzard buried Deepwater Horizon oil. *Nature*, 10.1038/nature.2013.12304.
- Baelum J, et al. (2012) Deep-sea bacteria enriched by oil and dispersant from the Deepwater Horizon spill. *Environ Microbiol* 14(9):2405–2416.
- Chanton JP, et al. (2012) Radiocarbon evidence that carbon from the Deepwater Horizon spill entered the planktonic food web of the Gulf of Mexico. *Environ Res Lett* 7(4):045303.
- Cherrier J, Sarkodee-Adoo J, Guilderson TP, Chanton JP (2014) Fossil carbon in particulate organic matter in the Gulf of Mexico following the Deepwater Horizon event. *Environmental Science and Technology Letters* 1(1):108–112.
- Passow U, Ziervogel K, Asper V, Diercks A (2012) Marine snow formation in the aftermath of the Deepwater Horizon oil spill in the Gulf of Mexico. *Environ Res Lett* 7(3):035301.
- Kujawinski EB, et al. (2011) Fate of dispersants associated with the deepwater horizon oil spill. *Environ Sci Technol* 45(4):1298–1306.
- Chakraborty R, Borglin SE, Dubinsky EA, Andersen GL, Hazen TC (2012) Microbial response to the MC-252 oil and Corexit 9500 in the Gulf of Mexico. *Front Microbiol* 3:357.
- Rivers AR, et al. (2013) Transcriptional response of bathypelagic marine bacterioplankton to the Deepwater Horizon oil spill. *ISME J* 7(12):2315–2329.
- Valentine DL, et al. (2012) Dynamic autoinoculation and the microbial ecology of a deep water hydrocarbon eruption. *Proc Natl Acad Sci USA* 109(50):20286–20291.
- Prince RC, et al. (1994) 17.alpha.(H)-21.beta.(H)-hopane as a conserved internal marker for estimating the biodegradation of crude oil. *Environ Sci Technol* 28(1):142–145.
- Aeppli C, et al. (2014) Recalcitrance and degradation of petroleum biomarkers upon abiotic and biotic natural weathering of Deepwater Horizon oil. *Environ Sci Technol* 48(12):6726–6734.
- Liu Y (2011) *Monitoring and Modeling the Deepwater Horizon Oil Spill: A Record-Breaking Enterprise* (American Geophysical Union, Washington, DC), pp vii, 271 pp.
- Paris CB, et al. (2012) Evolution of the Macondo well blowout: Simulating the effects of the circulation and synthetic dispersants on the subsea oil transport. *Environ Sci Technol* 46(24):13293–13302.
- Garcia-Pineda O, et al. (2013) Detection of floating oil anomalies from the Deepwater Horizon oil spill with synthetic aperture radar. *Oceanography (Wash DC)* 26(2):124–137.
- Le Hénaff M, et al. (2012) Surface evolution of the deepwater horizon oil spill patch: Combined effects of circulation and wind-induced drift. *Environ Sci Technol* 46(13):7267–7273.
- Mezić I, Loire S, Fonoberov VA, Hogan P (2010) A new mixing diagnostic and Gulf oil spill movement. *Science* 330(6003):486–489.
- Lindo-Atichati D, et al. (2014) Simulating the effects of droplet size, high-pressure biodegradation, and variable flow rate on the subsea evolution of deep plumes from the Macondo blowout. *Deep Sea Res Part II Top Stud Oceanogr*, 10.1016/j.dsr.2012.2014.1001.1011.
- Aeppli C, et al. (2012) Oil weathering after the Deepwater Horizon disaster led to the formation of oxygenated residues. *Environ Sci Technol* 46(16):8799–8807.
- Aeppli C, Reddy CM, Nelson RK, Kellermann MY, Valentine DL (2013) Recurrent oil sheens at the deepwater horizon disaster site fingerprinted with synthetic hydrocarbon drilling fluids. *Environ Sci Technol* 47(15):8211–8219.
- Carmichael CA, et al. (2012) Floating oil-covered debris from Deepwater Horizon: Identification and application. *Environ Res Lett* 7(1):015301.
- Mason OU, et al. (2014) Metagenomics reveals sediment microbial community response to Deepwater Horizon oil spill. *ISME J* 8(7):1464–1475.
- White HK, et al. (2012) Impact of the Deepwater Horizon oil spill on a deep-water coral community in the Gulf of Mexico. *Proc Natl Acad Sci USA* 109(50):20303–20308.
- Boehm PD, Carragher PD (2012) Location of natural oil seep and chemical fingerprinting suggest alternative explanation for deep sea coral observations. *Proc Natl Acad Sci USA* 109(40):E2647–E2647, author reply E2648.
- White HK, et al. (2012) Reply to Boehm and Carragher: Multiple lines of evidence link deep-water coral damage to Deepwater Horizon oil spill. *Proc Natl Acad Sci USA* 109(40):E2648–E2648.
- Fisher CR, et al. (2014) Footprint of Deepwater Horizon blowout impact to deep-water coral communities. *Proc Natl Acad Sci USA* 111(32):11744–11749.
- Montagna PA, et al. (2013) Deep-sea benthic footprint of the deepwater horizon blowout. *PLoS ONE* 8(8):e70540, 10.1371/journal.pone.0070540.
- Burdige DJ (2006) *Geochemistry of Marine Sediments* (Princeton Univ Press, Princeton, NJ).
- Yeager KM, Santschi PH, Rowe GT (2004) Sediment accumulation and radionuclide inventories (Pu-239,Pu-240, Pb-210 and Th-234) in the northern Gulf of Mexico, as influenced by organic matter and macrofaunal density. *Mar Chem* 91(1-4):1–14.